

Grafting pH-sensitive poly[2-(diethylamino)ethyl methacrylate] modification of vesicular silica with activator regenerated by electron transfer atom transfer radical polymerisation for controlled drug release

Fangfang Liu, Yan Zhang, Guowei Zhou

Key Laboratory of Fine Chemicals in Universities of Shandong, School of Chemistry and Pharmaceutical Engineering, Qilu University of Technology, Jinan 250353, People's Republic of China
E-mail: guoweizhou@hotmail.com

Published in Micro & Nano Letters; Received on 15th October 2014; Revised on 11th November 2014; Accepted on 3rd December 2014

pH-sensitive poly[2-(diethylamino)ethyl methacrylate]-modified vesicular silica (VS-PDEAEMA) is prepared in different amounts of 2-(diethylamino)ethyl methacrylate via activators regenerated by electron transfer for atom transfer radical polymerisation. The pH-responsive polymer is successfully grafted onto the shell of vesicular silica (VS) and then characterised. The inner PDEAEMA layer became thick, while the outmost polymer thickness did not change as the monomer amount was increased. Pure VS and VS-PDEAEMA are employed as supports for the loading and release of captopril. The release profiles of the captopril-loaded samples are studied in phosphate buffer solution with different pH values (4.0, 6.0 and 7.4). The captopril release rate can be controlled by PDEAEMA-functionalised carriers. Moreover, 31.5 and 70.0 wt% of captopril is released from the grafted polymer at pH 7.4 and 4.0, respectively. The modified VS can have potential applications in targeted drug delivery systems.

1. Introduction: Mesoporous silica nanoparticles (MSNs) have been widely used in enzyme catalysis [1], controlled drug release [2], protein separation [3], controlled dye release [4] and sensors [5] because of their large specific surface area and pore volume, low cytotoxicity and good biological adaptability. Recent studies have revealed that MSNs can serve as drug delivery systems for various therapeutic agents against several diseases, including bone/tendon tissue engineering [6], diabetes [7], inflammation [8] and cancer [9], because of their unique mesoporous structure.

Pure silica cannot achieve the desired effect of drug release and causes undesirable side effects to normal cells and organs [10]. Meanwhile, organic material-modified MSNs can effectively control drug release by responding to external stimuli. MSN-polymer composites have inorganic and organic material advantages [11]. The high surface area of silica imparts dimensional stability, and polymers possess chemical stability, adsorption or catalytic properties and stimuli-responsive properties [12]. Atom transfer radical polymerisation (ATRP) is a polymerisation technique commonly used to graft polymers onto MSNs [13]. Mei *et al.* [14] described the formation of diblock copolymer brushes comprising blocks of p(2-phenyl-1, 3-dioxan-5-yl methacrylate) (PDM) and pH-sensitive p(ethylene glycol) methyl ether methacrylate on the surface of hollow mesoporous silica (HMS) by ATRP. Yu *et al.* [15] successfully grafted pH-sensitive poly(N, N-dimethylaminoethyl methacrylate) (PDMAEMA) onto the surface of HMS via ATRP, with the HMS and the HMS-PDMAEMA having specific surface areas of 831.9 and 403.3 m²/g, respectively. Their experiment demonstrated that HMS-PDMAEMA can load substantial doxorubicin and have a good response to pH. Sun *et al.* [16] grafted poly[2-(diethylamino)ethyl methacrylate] (PDEAEMA) onto the surface of MSNs by surface-initiated ATRP. They found that MSN-PDEAEMA can control the release of Rhodamine B from the mesopores by adjusting the solution's pH. However, the conventional ATRP has some shortcomings, including a strict requirement for an anaerobic environment and large quantities of catalyst. To overcome these shortcomings, Jakubowski *et al.* [17] developed a new approach, that is, the activator regenerated by electron transfer ATRP (ARGET ATRP). ARGET ATRP can be conducted in sealed vials or jars without

deoxygenation. Cao *et al.* [18, 19] grafted PDMAEMA, poly(N-isopropylacrylamide), poly(methyl methacrylate) and polystyrene onto the surface of SBA-15 using ARGET ATRP. They demonstrated that ARGET ATRP is highly suitable for synthesising high surface area silica-polymer composites and those adjustable polymer loadings can achieve appreciable polymer film thicknesses. So, ARGET ATRP has emerged as a powerful method to synthesise well-defined polymer brushes in nanopores.

PDEAEMA is a pH-sensitive polymer with a pK_a of approximately 7.3; this polymer is applicable in many biomedical fields because of its low toxicity [20]. PDEAEMA has been shrunk to provide a secure encapsulation of species at neutral conditions and extended to release encapsulated drugs at acidic conditions [21]. In this Letter, we report a facile method of grafting a pH-responsive polymer, that is, PDEAEMA, onto the shell of vesicular silica (VS) with diameters of 50–100 nm and shell thicknesses of 2–5 nm by ARGET ATRP. The inner PDEAEMA layer became thick because of excess monomer polymerisation in the inner shell layers, while the outmost polymer thickness was not changed as the monomer amount was increased. Captopril was selected as a model drug to explore the difference in drug loading and release behaviour between VS and VS-PDEAEMA. The release profiles of the captopril-loaded samples were studied in phosphate buffer solution with different pHs (4.0, 6.0 and 7.4). Results indicated that the captopril release rate can be controlled by PDEAEMA-functionalised carriers at different pHs. To the best of our knowledge, this study is the first to modify the surface of VS with pH-responsive PDEAEMA.

2. Experimental: Captopril (>98%) was purchased from the Hebei Jingye Chemical Group Co. Ltd. Didodecyl dimethylammonium bromide (DDAB) (98%), 3-aminopropyltriethoxysilane (APTES) (99%), ethyl-2-bromoisobutyrate (EBiB) (>98%), 2-(diethylamino)ethyl methacrylate (DEAEMA) (99%) and 2-bromoisobutryl bromide (BiB) (97%) were purchased from Sigma-Aldrich (St. Louis, MO, USA). The monomer DEAEMA was purified by passing through an alumina column for inhibitor removal and then being subjected to vacuum distillation. FeCl₃·6H₂O (>99%), cetyltrimethylammonium bromide (CTAB)

($\geq 90.0\%$), tetraethoxysilane (TEOS) ($>99\%$), hydrofluoric acid (HF) (40%), triethylamine ($>99.0\%$), N,N-dimethylformamide (DMF) and ascorbic acid (VC) ($>99.7\%$) were purchased from Sinopharm Chemical Reagent Co. Ltd (China). Triphenylphosphine (PPh_3) ($>99\%$), toluene, tetrahydrofuran (THF), toluene and all other chemicals were of analytical grade and obtained from the Tianjin Chemical Agent Company (China). Deionised water was used in all experiments.

VS was synthesised using a hydrothermal method according to our previous study [22]. CTAB (0.140 g) was dissolved in 35.0 ml of deionised water with continuous stirring at 35°C to form a clear solution. The solution was added with DDAB (0.150 g) and then with $\text{NH}_3\cdot\text{H}_2\text{O}$ (0.7 ml) upon complete dissolution of DDAB. After 2 h, 2.000 g of TEOS was added dropwise to the solution under vigorous stirring. The reaction solution was constantly stirred at 35°C for 24 h, transferred into a Teflon-lined autoclave, heated and then stored at 100°C for 24 h under static conditions. Finally, the white solid products were collected by filtration, washed with water, dried under vacuum at room temperature and then calcined at 550°C for 6 h to remove the surfactant template.

Amino-functionalised VS (VS-NH_2) was prepared as follows. VS (0.410 g) was dispersed in 20.0 ml of dry toluene. The solution was added with APTES (0.1 ml) and then stirred at 75°C under N_2 atmosphere for 18 h. The nanoparticles were collected by centrifugation, washed thoroughly with ethanol and toluene and then dried under vacuum at room temperature.

Br-modified VS (VS-Br) was also prepared as follows. VS-NH_2 (0.730 g), toluene (20.0 ml) and triethylamine (1.0 ml) were added into a 100 ml flask. BiB (1.5 ml) in 5.0 ml of toluene was added dropwise into the mixture at 0°C under N_2 atmosphere. The mixture was stirred for 1 h at 0°C , the flask was removed to ambient temperature, and then the mixture was stirred again for 12 h. The product was separated by centrifugation, washed five times with toluene and then dried under vacuum at 40°C .

In a typical process, 0.080 g of VS-Br , 0.044 g of PPh_3 , 0.005 g of $\text{FeCl}_3\cdot 6\text{H}_2\text{O}$, 24.0 μl of EBiB and DEAEMA with different amounts (9.7, 11.3 and 13.0 ml) were dispersed in 15.0 ml of dried DMF in a 100 ml flask. The mixture was degassed by bubbling under N_2 for 30 min. The flask was then sealed. A mixture of 0.029 g of VC and 3.0 ml of DMF was slowly added into the flask. The flask was moved into an oil bath at 60°C with stirring. After 22 h, the flask was opened, and the reaction was terminated. The product was collected by centrifugation, washed with THF and then dried. The molar ratio of $\text{FeCl}_3\cdot 6\text{H}_2\text{O}:\text{PPh}_3:\text{DEAEMA}:\text{EBiB}:\text{VC}$ was 0.1:1:(292, 342, 392):1:1. The resulting products were designated as SM1, SM2 and SM3, representing the different added amounts of DEAEMA.

VS-PDEAEMA (0.030 g) was dispersed in 10.0 ml of THF in a PTFE vessel. HF (1.5 ml) was added, and the suspension was stirred for 12 h at room temperature. The suspension was neutralised with an aqueous solution of Na_2CO_3 [16]. The product was separated by centrifugation and then dried under vacuum at 40°C . PDEAEMA was used for ^1H nuclear magnetic resonance (^1H NMR) measurement.

Captopril was dissolved in phosphate buffer saline at pH 4.0 with a concentration of 20 mg/ml. SM3 or VS (0.075 g) was immersed in 25.0 ml of captopril solution at room temperature with stirring for three days. The SM3-loaded captopril (SM3-cap) or VS-loaded captopril (VS-cap) was collected by centrifugation, washed extensively with deionised water and then dried under vacuum overnight. The drug loading content and entrapment efficiency were calculated using the following equations [15]:

$$\text{Loading content (wt\%)} = \frac{\text{Weight of drug in VS}}{\text{Weight of drug loaded VS}}$$

$$\text{Entrapment efficiency (wt\%)} = \frac{\text{Weight of drug in VS}}{\text{Initial weight of drug}}$$

50.0 ml of aqueous solutions at different pHs (4.0, 6.0 and 7.4) were then stirred at the same rate. At timed intervals, 3.0 ml of the mixture was withdrawn, and 3.0 ml of the fresh phosphate buffer solution was added. The mixture was centrifuged. The supernatant liquids were withdrawn for monitoring using a UV-vis spectrophotometer at an absorbance wavelength of 207 nm.

Field-emission scanning electron microscopy (FESEM) was conducted using a SUPRATM 55 microscope operated at 5 kV. Powder products were dispersed in ethanol by sonication for 10 min. They were dropped onto the surface of an Si wafer and then dried at 60°C overnight. The specimens were coated with a layer of Au by ion sputtering and then observed via scanning electron microscopy. For high-resolution transmission electron microscopy (HRTEM), the powder products were dispersed in ethanol by sonication for 10 min and then placed on C-coated Cu grids. After drying at 60°C overnight, the products were observed on a JEM-2100 at an accelerating voltage of 200 kV. N_2 adsorption-desorption experiments were performed by a TriStar 3020. The surface area and pore size distribution were estimated via Brunauer-Emmett-Teller (BET) and Barrett-Joyner-Halenda (BJH) methods using adsorption isotherms. Fourier-transform infrared (FTIR) spectra were obtained using a BRUKER TENSOR 27 spectrometer at $400\text{--}4000\text{ cm}^{-1}$. Compressed KBr pellets that contained approximately 1 wt% of the sample were used. Thermogravimetric analysis (TGA) was conducted using a TGA 1500 DSP-SP instrument with a heating rate of $10^\circ\text{C}/\text{min}$ from room temperature to 800°C under N atmosphere. The ^1H NMR spectrum of the obtained polymer was recorded using a Bruker AVANCE II 400 MHz NMR instrument with CDCl_3 as the solvent and tetramethylsilane as an internal standard. The absorbance of captopril was obtained using a SHIMADZU UV-2600 spectrophotometer.

3. Results and discussion: VS-PDEAEMA was prepared according to Fig. 1. VS-NH_2 was prepared by reacting the silanol on the surface of VS with the oxethyls of APTES. Then, VS-Br was obtained by reacting the 2-bromoisobutryl group of BiB with the amino groups in VS-NH_2 . Finally, VS-PDEAEMA was obtained via ARGET ATRP in the system, which consisted of VS-Br as the initiator, $\text{FeCl}_3\cdot 6\text{H}_2\text{O}$ as the catalyst, PPh_3 as the ligand, VC as the reducing agent and DEAEMA as the monomer.

Fig. 2 shows the HRTEM images of VS, SM1, SM2 and SM3. The hydrothermally synthesised VS has diameters of 50–100 nm, shell thicknesses of 2–5 nm and interlamellar voids of 2–3 nm (Fig. 2a). The numbers of layers of VS are estimated to be three to four (Fig. 2a). The outermost shell thickness of VS is approximately 5 nm. The VS-PDEAEMA maintains the VS structure and the outermost shell thicknesses of SM1, SM2 and SM3 are all approximately 9 nm, which preliminarily confirms the successful polymer grafting. With the increase in the monomer amount, the outermost shell thicknesses of SM1, SM2 and SM3 do not change and the interlamellar voids become small (Figs. 2b–d) because of excess monomer polymerisation in the inner layers. Compared with that of the outer layer, the polymer thickness of the inner layer becomes thin. This result indicates that the outer layers confine the monomer that enters the inner layers.

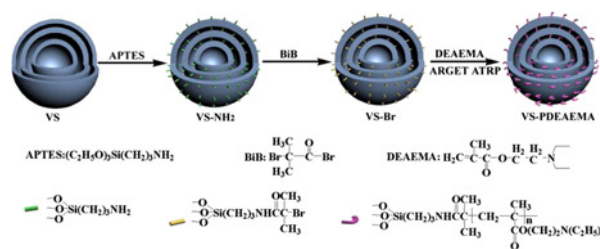


Figure 1 Schematic of VS-PDEAEMA formation by ARGET ATRP

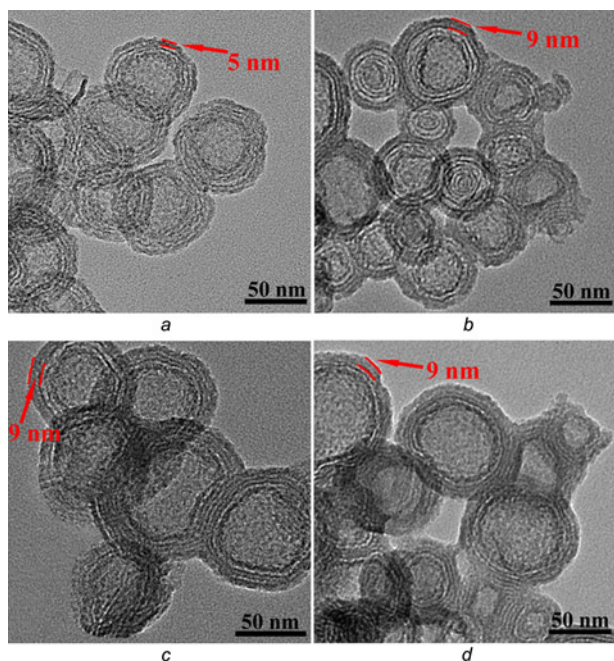


Figure 2 HRTEM images

a VS
b SM1
c SM2
d SM3

Fig. 3 shows the FESEM images of VS and SM3. As shown in the HRTEM (Fig. 2) and the FESEM (Fig. 3) images, the transformation efficiency of VS powders from the method is almost 100%, although several particles were broken. Comparison of the FESEM images before (Fig. 3a) and after (Fig. 3b) polymerisation reveals that the diameter of SM3 is large and that the edges of SM3 are blurred. This result indicates the successful grafting of the polymer onto the outmost shell of VS. With the increase in the monomer amount, the polymer layer thickness does not considerably change (Fig. 3b).

The FTIR spectra of VS, VS-NH₂, VS-Br, SM1, SM2 and SM3 are shown in Fig. 4. Fig. 4, spectra *a* shows a broad absorption peak at 3750–3000 cm⁻¹, which is attributed to the stretching vibration of the silanol group. The absorption peak at 950 cm⁻¹ is associated with Si–OH asymmetric bending vibrations. A new adsorption peak in comparison with VS at 1530 cm⁻¹ is the typical absorption peak of NH₂ present on the surface of VS-NH₂ (Fig. 4, spectra *b*) [23, 24]. The peaks at 2900, 1280 and 1380 cm⁻¹ (Fig. 4, spectra *c*) are attributed to the C–H stretching vibrations and C–H bending vibrations of methyl groups, indicating the successful attachment

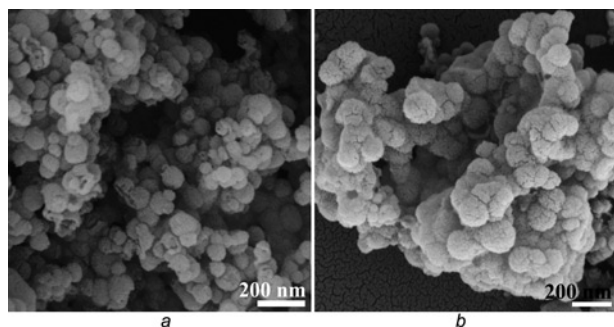


Figure 3 FESEM

a VS
b SM3

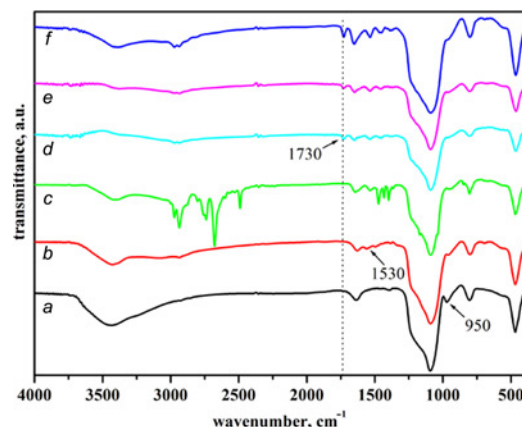


Figure 4 FTIR spectra

a VS; b VS-NH₂; c VS-Br; d SM1; e SM2; f SM3

of the 2-bromoisobutryl group to VS-NH₂. The absorption bands at 1730 cm⁻¹ in Figs. 4, spectra *d–f* correspond to the stretching vibration of the ester carbonyl group in PDEAEMA, suggesting the successful grafting of PDEAEMA to VS-Br [16].

The TGAs of VS, VS-NH₂, VS-Br, SM1, SM2 and SM3 were performed after vacuum-drying the samples at 40°C for 48 h. Fig. 5 shows that the weight losses of VS, VS-NH₂, VS-Br, SM1, SM2 and SM3 are 5.16, 17.36, 21.39, 32.59, 36.94 and 44.16%, respectively, when the samples were heated to 800°C. A 4.03% difference in weight loss was detected between VS-NH₂ and VS-Br at 800°C. The differences in weight loss between VS-Br and VS-PDEAEMA are 11.20% (SM1), 15.55% (SM2) and 22.77% (SM3). These results prove the successful grafting of PDEAEMA onto the surface of VS. These results indicate that the weight loss of VS-PDEAEMA increases with increasing monomer amounts.

The structure of PDEAEMA was confirmed by ¹H NMR, as shown in Fig. 6. The signal at 0.85 ppm was ascribed to the methyl protons adjacent to the main chain. The chemical shift of six protons of N(CH₂CH₃)₂ chain ends was found at 1.20 ppm. The peak at 2.04 ppm corresponds to the methylene protons in the backbone. The peaks at 2.60 and 2.75 ppm correspond to the methylene adjacent to N in DEAEMA units (Fig. 6). The proton signal at 4.05 ppm can be assigned to the methylene protons adjacent to O in DEAEMA [25]. These results reveal the successful synthesis of PDEAEMA by ARGET ATRP.

N₂ adsorption–desorption isotherms were employed to measure the pore structures of the samples. The BET isotherm of VS

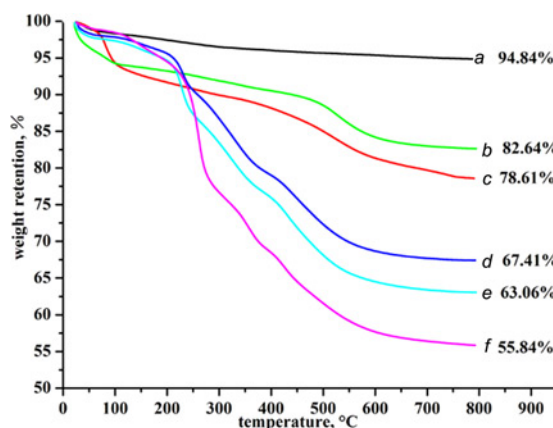


Figure 5 TGA results

a VS; b VS-NH₂; c VS-Br; d SM1; e SM2; f SM3

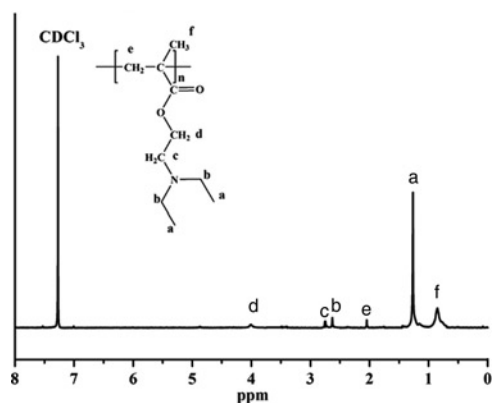


Figure 6 ^1H NMR spectrum of PDEAEMA

(Fig. 7) exhibits the characteristic type-IV N_2 adsorption–desorption pattern with H4-type hysteresis loops associated with capillary condensation at high relative pressures [22]. The BJH pore size distribution of VS is narrow, as shown in the inset of Fig. 7. The BET isotherms of SM1, SM2 and SM3 in Fig. 7 demonstrate that the mesopores are inaccessible to N_2 gas. PDEAEMA is grafted onto the inner layer shell of VS, and the compact polymer layers on the outer surface of VS prevent N_2 penetration [19]. Table 1 summarises the pore structures of VS, SM1, SM2, SM3, VS-cap and SM3-cap. The surface area (S_{BET}), pore volume (V) and average pore diameter (D) of VS are $618.5 \text{ m}^2/\text{g}$, $0.95 \text{ cm}^3/\text{g}$ and 2.55 nm , respectively. The S_{BET} and V of SM1, SM2 and SM3 decrease after polymerisation. When the quantity of DEAEMA is increased, S_{BET} and V decrease. Specifically, S_{BET} is decreased to 40.1 , 37.6 and $33.0 \text{ m}^2/\text{g}$ and V to 0.34 , 0.33 and $0.30 \text{ cm}^3/\text{g}$ because of excess monomer polymerisation in the interlamellar voids. These results are in accordance with the transmission electron microscopy results.

N_2 adsorption–desorption isotherms were measured for the pore structures of captopril-loaded VS and SM3 (Fig. 8). The BJH pore size distribution of VS-cap is narrow, as shown in the inset of Fig. 8. The BET isotherm of VS-cap exhibits the characteristic type-IV N_2 adsorption–desorption pattern, which is similar to that of VS (Fig. 7). The BET isotherm of SM3-cap is similar to that of SM3. Therefore, the structure and pore shape of the supporting materials are not significantly changed after captopril loading. Compared with that of VS, the D of VS-cap is decreased to 2.30 (Table 1). The S_{BET} and V of VS-cap and SM3-cap are lower compared with those of the corresponding support samples, indicating that captopril is mostly loaded into the interlamellar voids of VS. The captopril loading contents of VS-cap and SM3-cap are

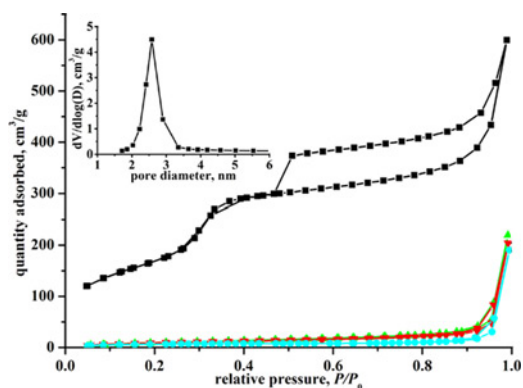


Figure 7 N_2 adsorption–desorption isotherms of VS (black squares) SM1 (green triangle), SM2 (red down-pointing triangle) and SM3 (blue circle) Inset is BJH pore size distribution plot of VS

Table 1 Mesopore parameters of VS, SM1, SM2, SM3, VS-cap and SM3-cap

Sample	$S_{\text{BET}}, \text{m}^2/\text{g}$	$V, \text{cm}^3/\text{g}$	D, nm
VS	618.5	0.95	2.55
SM1	40.1	0.34	^a
SM2	37.6	0.33	^a
SM3	33.0	0.30	^a
VS-cap	278.5	0.50	2.30
SM3-cap	28.9	0.20	^a

^aMesopores were not accessible to nitrogen gas

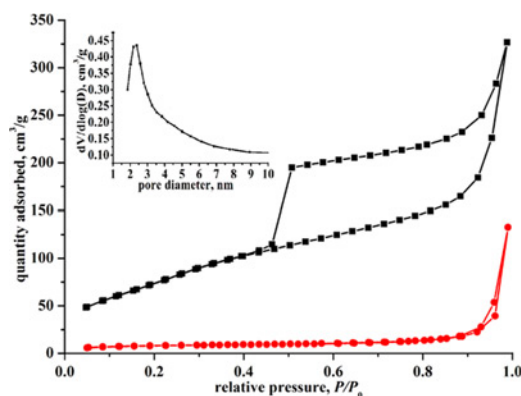


Figure 8 N_2 adsorption–desorption isotherms of VS-captopril (black squares), SM3-captopril (red circle) Inset is BJH pore size distribution plot of the VS-captopril

approximately 26.0 and $43.0 \text{ wt}\%$, respectively. The entrapment efficiencies of VS-cap and SM3-cap are estimated to be 30.0 and $50.0 \text{ wt}\%$, respectively. After modification with PDEAEMA, the loading content obviously increases. This result can be attributed to the fact that drugs can be stored not only in the interlamellar voids of supports but also in the hydrophobic PDEAEMA layer of SM3 [13].

The in-vitro drug release behaviour of VS-cap and SM3-cap was studied in phosphate buffer saline with different pHs (4.0 , 6.0 and 7.4) at room temperature and then stirred at the same rate. The captopril release curves at different pHs are shown in Fig. 9. The captopril released from VS-cap is $20.0 \text{ wt}\%$ at pH 4.0 , $14.0 \text{ wt}\%$ at pH 6.0 and $12.8 \text{ wt}\%$ at pH 7.4 . These data show that the release amount is small and that the difference in release amount between different pHs is not significant. The drug release rate at

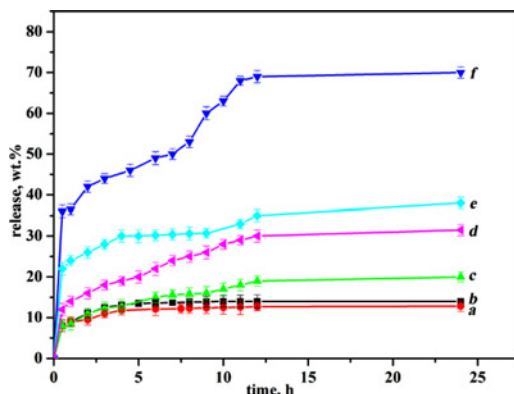


Figure 9 Captopril release from VS-cap and from SM3-cap a pH 7.4 ; b pH 6.0 ; c pH 4.0 Captopril release from SM3-cap d pH 7.4 ; e pH 6.0 ; f pH 4.0

pH 4.0 is slightly higher than that at pH 6.0 and 7.4. This result may be attributed to the relatively weaker H bond interaction between the drug molecule and the releasing media at pH 4.0 than at pH 6.0 and 7.4 [26]. Fig. 9 shows that the amount of drug release of SM3-cap is pH dependent; that is, it obviously increases with decreasing pH. The cumulative amount of drug release could reach up to 70.0 wt% after 24 h at pH 4.0, which is significantly higher than that at pH 6.0 (38.0 wt%) and 7.4 (31.5 wt%). This result can be attributed to the fact that more PDEAEMA is protonated with decreasing pH and that the polymer chains are fully extended because of the electrostatic repulsions between PDEAEMA chains [21]; thus, a larger amount of captopril is released at pH 4.0 than at pH 6.0 and 7.4. VS-PDEAEMA shrinks PDEAEMA under neutral conditions because PDEAEMA is a hydrophobic polymer. The shrunken PDEAEMA should seal the pores in the VS shells. Consequently, only a small amount of captopril is released. The aforementioned results show that the amount of captopril released depends on the solution's pH. Therefore, VS-PDEAEMA controls the drug release by changing the solution's pH.

4. Conclusion: We prepared pH-sensitive VS-PDEAEMA by using a facile ARGET ATRP method. With increasing monomer amounts, the interlamellar voids are narrowed, and the outmost shell thicknesses of SM1, SM2 and SM3 are maintained at 9 nm. VS and SM3 were employed as supports for the loading and controlled release of captopril. The drug loading contents of SM3 are higher than those of VS. At pH 4.0 and 7.4, the amounts of captopril released by SM3-cap are 70.0 and 31.5 wt%, respectively. PDEAEMA is protonated, and the polymer is extended because of the electrostatic repulsions between PDEAEMA chains at pH 4.0. At pH 7.4, the polymer is in the collapsed state because of the hydrophobic interaction of polymer chains. The pH-responsive PDEAEMA layer anchored on VS can serve as a switch to control the opening and closing of the pores. This material could have potential applications in cancer therapy because of its pH sensitivity.

5. Acknowledgments: This work was supported by the National Natural Science Foundation of China (grant nos. 20976100, 51372124), the Natural Science Foundation of Shandong Province (grant no. ZR2011BQ009) and the Program for Scientific Research Innovation Team in Colleges and Universities of Shandong Province.

6 References

- [1] Hartmann M.: 'Ordered mesoporous materials for bioadsorption and biocatalysis', *Chem. Mater.*, 2005, **17**, pp. 4577–4593
- [2] Wang S.B.: 'Ordered mesoporous materials for drug delivery', *Microporous Mesoporous Mater.*, 2009, **117**, pp. 1–9
- [3] Chen L.H., Zhu G.S., Zhang D.L., *ET AL.*: 'Novel mesoporous silica spheres with ultra-large pore sizes and their application in protein separation', *J. Mater. Chem.*, 2009, **19**, pp. 2013–2017
- [4] Zhu Y.F., Jian D.L., Wang S.L.: 'Investigation of loading and release of guest molecules from hollow mesoporous silica spheres', *Micro Nano Lett.*, 2011, **6**, pp. 802–805
- [5] Melde B.J., Johnson B.J., Charles P.T.: 'Mesoporous silicate materials in sensing', *Sensors*, 2008, **8**, pp. 5202–5228
- [6] Tang F.Q., Li L.L., Chen D.: 'Mesoporous silica nanoparticles: synthesis, biocompatibility and drug delivery', *Adv. Mater.*, 2012, **24**, pp. 1504–1534
- [7] Zhao Y.N., Trewyn B.G., Slowing I.I., Lin V.S.Y.: 'Mesoporous silica nanoparticle-based double drug delivery system for glucose-responsive controlled release of insulin and cyclic AMP', *J. Am. Chem. Soc.*, 2009, **131**, pp. 8398–8400
- [8] Moularia B., Pertuita D., Pellequera Y., Lamprecht A.: 'The targeting of surface modified silica nanoparticles to inflamed tissue in experimental colitis', *Biomaterials*, 2008, **29**, pp. 4554–4560
- [9] Lu J., Liong M., Li Z.X., Zink J.I., Tamanoi F.: 'Biocompatibility, biodistribution, and drug delivery efficiency of mesoporous silica nanoparticles for cancer therapy in animals', *Small*, 2010, **6**, pp. 1794–1805
- [10] Azaïs T., Pételil C.T., Aussenac F., *ET AL.*: 'Solid-state NMR study of ibuprofen confined in MCM-41 material', *Chem. Mater.*, 2006, **18**, pp. 6382–6390
- [11] Li C.M., Yang J., Wang P.Y., Liu J., Yang Q.H.: 'An efficient solid acid catalyst: poly-p-styrenesulfonic acid supported on SBA-15 via surface-initiated ATRP', *Microporous Mesoporous Mater.*, 2009, **123**, pp. 228–233
- [12] Tsujii Y., Ohno K., Yamamoto S., Goto A., Fukuda T.: 'Structure and properties of high-density polymer brushes prepared by surface-initiated living radical polymerization', *Adv. Polym. Sci.*, 2006, **197**, pp. 1–45
- [13] Lay C.L., Tan H.R., Lu X.H., Liu Y.: 'pH-responsive poly(methacrylic acid)-grafted hollow silica vesicles', *Chem. Eur. J.*, 2011, **17**, pp. 2504–2509
- [14] Mei X., Chen D.Y., Li N.J., *ET AL.*: 'Hollow mesoporous silica nanoparticles conjugated with pH-sensitive amphiphilic diblock polymer for controlled drug release', *Microporous Mesoporous Mater.*, 2012, **152**, pp. 16–24
- [15] Yu F.Q., Tang X.D., Pei M.S.: 'Facile synthesis of PDEAEMA-coated hollow mesoporous silica nanoparticles and their pH-responsive controlled release', *Microporous Mesoporous Mater.*, 2013, **173**, pp. 64–69
- [16] Sun J.T., Hong C.Y., Pan C.Y.: 'Fabrication of PDEAEMA-coated mesoporous silica nanoparticles and pH-responsive controlled release', *J. Phys. Chem. C*, 2010, **114**, pp. 12481–12486
- [17] Jakubowski W., Min K., Matyjaszewski K.: 'Activators regenerated by electron transfer for atom transfer radical polymerization of styrene', *Macromolecules*, 2006, **39**, pp. 39–45
- [18] Cao L., Man T., Zhuang J.Q., Kruk M.: 'Poly (N-isopropylacrylamide) and poly(2-(dimethylamino)ethyl methacrylate) grafted on an ordered mesoporous silica surface using atom transfer radical polymerization with activators regenerated by electron transfer', *J. Mater. Chem.*, 2012, **22**, pp. 6939–6946
- [19] Cao L., Kruk M.: 'Grafting of polymer brushes from nanopore surface via atom transfer radical polymerization with activators regenerated by electron transfer', *Polym. Chem.*, 2010, **1**, pp. 97–101
- [20] Yusa S., Sugahara M., Endo T., Morishima Y.: 'Preparation and characterization of a pH-responsive nanogel based on a photo-cross-linked micelle formed from block copolymers with controlled structure', *Langmuir*, 2009, **25**, pp. 5258–5265
- [21] Lobb E.J., Ma I., Billingham N.C., Armes S.P.: 'Facile synthesis of well-defined, biocompatible phosphorylcholine-based methacrylate copolymers via atom transfer radical polymerization at 20°C', *J. Am. Chem. Soc.*, 2001, **123**, pp. 7913–7914
- [22] Zhang Y., Zhou G.W., Sun B., Zhao M.N., Zhang J.Y., Chen F.J.: 'A cationic-cationic co-surfactant templating route for synthesizing well-defined multilamellar vesicular silica with an adjustable number of layers', *Chem. Commun.*, 2014, **50**, pp. 2907–2909
- [23] Zhang L., Zhou G.W., Sun B., Chen F.J., Zhao M.N., Li T.D.: 'Tunable shell thickness in silica nanospheres functionalized by a hydrophobic PMMA-PSt diblock copolymer brush via activators generated by electron transfer for atom transfer radical polymerization', *Macromol. Chem. Phys.*, 2013, **214**, pp. 1602–1611
- [24] Zhao M.N., Zhou G.W., Zhang L., Li X.Y., Li T.D., Liu F.F.: 'Fabrication and photoactivity of a tunable-void SiO₂-TiO₂ core-shell structure on modified SiO₂ nanospheres by grafting an amphiphilic diblock copolymer using ARGET ATRP', *Soft Mat.*, 2014, **10**, pp. 1110–1120
- [25] Gao C., Li W.W., Morimoto H., Nagaoka Y., Maekawa T.: 'Magnetic carbon nanotubes: synthesis by electrostatic self-assembly approach and application in biomanipulations', *J. Phys. Chem. B*, 2006, **110**, pp. 7213–7220
- [26] Qu F.Y., Zhu G., Huang S.S., *ET AL.*: 'Controlled release of captopril by regulating the pore size and morphology of ordered mesoporous silica', *Microporous Mesoporous Mater.*, 2006, **92**, pp. 1–9